

### Key Points:

- The Bohai Sea, Japan Sea, Beibu Bay, and east of Taiwan Island have the highest mean annual total days
- Severe MHWs in the Bohai Sea could have impacted fishery resources and occurrence of harmful algal blooms
- In the future, 2040 is a key node for the future changes of MHW under different RCPs

### Supporting Information:

- Supporting Information S1

### Correspondence to:

X. Zou,  
zouxq@nju.edu.cn

### Citation:

Yao, Y., Wang, J., Yin, J., & Zou, X. (2020). Marine heatwaves in China's marginal seas and adjacent offshore waters: Past, Present, and Future. *Journal of Geophysical Research: Oceans*, 125, e2019JC015801. <https://doi.org/10.1029/2019JC015801>

Received 21 OCT 2019

Accepted 19 FEB 2020

Accepted article online 21 FEB 2020

Corrected 17 MAR 2020

This article was corrected on 17 MAR 2020. See the end of the full text for details.

## Marine Heatwaves in China's Marginal Seas and Adjacent Offshore Waters: Past, Present, and Future

Yulong Yao<sup>1,2</sup> , Junjie Wang<sup>3</sup> , Jianjun Yin<sup>4</sup> , and Xinqing Zou<sup>1,2</sup> 

<sup>1</sup>School of Geographic and Oceanographic Sciences, Nanjing University, Nanjing, China, <sup>2</sup>Ministry of Education Key Laboratory for Coastal and Island Development, Nanjing University, Nanjing, China, <sup>3</sup>Key Laboratory of Marine Chemistry Theory and Technology, Ministry of Education, Ocean University of China, Qingdao, China, <sup>4</sup>Department of Geosciences, University of Arizona, Tucson, AZ, USA

**Abstract** Under the combined impacts of natural changes and human activities, the past, current, and future marine heatwaves (MHWs) in China's marginal seas and adjacent offshore waters (CMSOW) need a comprehensive understanding. This study provides a systematic analysis of the spatiotemporal variations using daily sea surface temperature data and simulates the future trend using 12 climate models. During 1982–2018, the mean annual total days, duration, frequency, and mean intensity of the MHWs in the CMSOW increased by 20–30 days/decade, 5–9 days/decade, 1–2 decade<sup>-1</sup>, and 0.1–0.3°C/decade, respectively ( $p < 0.01$ ). The maximum sea surface temperature anomalies in the Bohai Sea was over 6–8°C, and the MHW's frequency, duration, and mean intensity were higher than twice the global average, which could have impacted fishery resources and occurrence of harmful algal blooms. The variations of the MHWs in the CMSOW result from the robust ocean surface warming, which is caused by increased solar radiation due to reduced cloud cover, reduced ocean heat loss from weaker wind speed, weakening but warmer Kuroshio, and strong El Niño. In the future, the areas with longer total days and duration will increase; the spatial pattern of frequency has a negative relationship with that of duration while that of mean intensity is mostly unchanged. Year 2040 is a key node for the future changes of MHW under different Representative Concentration Pathways. The trend of total days increases from fast to slow, and frequency shows an opposite trend; the duration and mean intensity rise faster after 2040.

### 1. Introduction

Human-induced global warming can lead to more frequent and intense heatwaves on land, thus exerting significant impacts on human health and regional economies (Meehl & Tebaldi, 2004; Stott et al., 2004). As most of the excess heat is stored in the ocean, the global ocean has also experienced extreme warming events (Lima & Wethey, 2012). Land heatwaves have been intensively studied during the past decades; marine heatwaves (MHWs), however, have started to draw scientific and public attention only in recent years (Holbrook et al., 2019). Thus far, different definitions of MHWs have been proposed (Maynard et al., 2008; Sorte et al., 2010; Selig et al., 2010). Among them, the one defined by Hobday et al. (2016) has been widely used: a MHW is an anomalously warming event lasting for at least 5 days with daily temperatures higher than the 90th percentile over a 30-year historical baseline period. Based on this definition, MHWs that occur in different regions can be directly compared (Manta et al., 2018).

The global ocean temperatures have increased in most regions of the world over the past century, leading to longer and more frequent MHWs (Oliver et al., 2018; Smale et al., 2019). A recent global analysis identified that the regions with large sea surface temperature (SST) variability, especially controlled by the western boundary current (WBC) extension, are the hotspots of MHWs (Hu et al., 2015; Oliver et al., 2018). During the austral summer of 2015/2016, SSTs off southeast Australia were the warmest on record, reaching up to 3–4°C above climatological means (Oliver, Benthuysen, et al., 2017). In austral summer 2017, the southwestern Atlantic shelf also experienced the most intense warming event with temperature reaching 26.8°C, 1.7°C above the previous maximum (Manta et al., 2018). During 1958–2014, the SST in the East China Sea increased by ~1.71°C at a rate of 0.3°C per decade during winter and by ~0.86°C at a rate of 0.15°C per decade during summer, and its warming rate were greater than the global mean since the 1980s (Cai et al., 2017). The potential physical drivers of some high-profile

MHWs were also discussed in previous studies, and the occurrence of MHWs were related to different local processes including atmospheric forcing, ocean stratification, and warm water through oceanic currents, and also to atmospheric teleconnections associated with global modes of variability including El Niño Southern Oscillation and Pacific Decadal Oscillation (Chen et al., 2014; Feng et al., 2013; Holbrook et al., 2019; Myers et al., 2018; Oliver, Perkins-Kirkpatrick, et al., 2017).

The damaging consequences of MHWs and their influences on the structure of marine communities and sustainability of ecosystems have been reported (Garrabou et al., 2009; Cavole et al., 2016; Oliver et al., 2017; Wernberg et al., 2016). In early 2011, the MHWs along the west coast of Australia resulted in an entire regime shift of the temperate reef ecosystem including a reduction in the abundance of habitat-forming seaweeds and a subsequent shift in fish community structure toward tropicalization (Wernberg et al., 2013, 2016). In 2013, the warm blob in the northeast Pacific contributed to continued low chlorophyll biomass (Jacox et al., 2016), and harmful algal blooms (HABs) extending from California to Alaska and unusual deaths of marine mammals and seabirds were observed (Cavole et al., 2016; Di Lorenzo & Mantua, 2016; Jones et al., 2018; McCabe et al., 2016; Whitney, 2015). The study by Frölicher et al. (2018) revealed that more frequent and extreme MHWs in response to global warming could potentially push marine organisms and ecosystems to or even beyond the limits of their resilience. In addition, evidence has shown that the MHWs in coastal waters could be even more harmful to shallow water ecosystems than to marine ecosystems in open oceans (Schlegel et al., 2017). Substantial deaths of over 25 macro-benthic invertebrate species were found in the Northwestern Mediterranean area during the period with anomalous SSTs in the summer of 2013 (Garrabou et al., 2009). High fish mortalities and a toxic HAB in the capital city of Uruguay occurred during the anomalous warming in the Southwestern Atlantic shelf in 2017 (Manta et al., 2018).

China's marginal seas are of abundant fishery resources and important ecological functions (Luo, 2016). Currently, 86 state-level marine ranching demonstration zones have been built across China's marginal seas and 178 national marine ranching demonstration zones are planned to be built by 2025 (Ministry of Agriculture of the PR China, 2017). However, the marine ranching ecosystems may be facing various risks and even large-scale seasonal deaths of organisms due to high temperature and low dissolved oxygen (DO) under the impacts of global warming (Liu et al., 2014; Yang et al., 2019). In the August of 2018, the unusually sharp increase in the SST in Dalian, Liaoning province, was observed to have caused the substantial deaths of the cultured sea cucumbers locally and a direct economic loss of more than US \$1 billion (Tencent News, 2018).

Considering the potential impacts of MHWs on marine ecosystems and economic development, a detailed investigation of the historical and current MHW properties in China's marginal seas is urgently needed. In this study, we used satellite observation data to study the characteristics of MHWs in China's marginal seas and adjacent offshore waters (CMSOW) over the past four decades. Furthermore, we explored their future projections by 2100 with a set of climate models under greenhouse-gas emission scenarios and discuss the physical drivers and potential ecological impacts of MHWs.

## 2. Material and Methods

### 2.1. Study Area

Our study area, the CMSOW, ranges from 0 to 42°N latitude and from 98 to 135°E longitude (Figure S1 in the supporting information), including China's marginal seas (i.e., from north to south, the Bohai Sea, Yellow Sea, East China Sea, and South China Sea) and adjacent offshore waters such as the Japan Sea and east of Taiwan Island. China's coastline stretches  $1.8 \times 10^4$  km from temperate and subtropical to tropical zones, and more than 42% of China's population resides in this coastal zone (Luo, 2016). The Bohai Sea to the north is shallow (with an average depth of 18m), semienclosed, and the only inland sea in China. It has three bays: Liaodong, Bohai, and Laizhou bay (Figure S1). The Yellow Sea and the East China Sea to the east are characterized by a broad continental shelf. In the southernmost South China Sea, many tropical coral reefs are distributed. The Kuroshio, the strong WBC flowing across this area, modulates regional climate by transporting excess heat northward from the tropics and affects typhoon development, fishery economy, and ocean circulation in surrounding marginal seas.

**Table 1***The Observational and Reanalysis Data Sets Used in the Present Study*

	Data set	Institute	Resolution	Period	Reference	Website
SST	OISST	NOAA ESRL	0.25°× 0.25°	1982–2018	(Reynolds et al., 2007)	<a href="https://www.esrl.noaa.gov/psd/">https://www.esrl.noaa.gov/psd/</a>
	HadISST1	UK Met Office Hadley Centre	1°× 1°	1979–2018	(Rayner et al., 2003)	<a href="https://www.metoffice.gov.uk/hadobs/hadisst/">https://www.metoffice.gov.uk/hadobs/hadisst/</a>
	COBE SST2	NOAA ESRL	1°× 1°	1979–2017	(Hirahara et al., 2014)	<a href="https://www.esrl.noaa.gov/psd/">https://www.esrl.noaa.gov/psd/</a>
ERA5	ERA5	ECMWF	0.25°× 0.25°	1982–2018	(Hersbach et al., 2018)	<a href="https://www.ecmwf.int/en/forecasts/datasets/reanalysis-datasets/era5">https://www.ecmwf.int/en/forecasts/datasets/reanalysis-datasets/era5</a>
Ocean Current	CORA1	NMSDSSP	0.5°× 0.5°	1982–2017	(Han et al., 2013)	<a href="http://mds.nmdis.org.cn/web/site/index_view">http://mds.nmdis.org.cn/web/site/index_view</a>

Abbreviations: COBE: Centennial in situ Observation-Based Estimates; CORA1; China Ocean Reanalysis version 1; ECMWF: European Centre for Medium-Range Weather Forecasts; ESRL, Earth System Research Laboratory; HadISST1: Hadley Centre Sea Ice and Sea Surface Temperature version 1; NMSDSSP, National Marine Science Data Sharing Service Platform of China; NOAA: National Oceanic and Atmospheric Administration; SST: sea surface temperature; OISST: Optimum Interpolation Sea Surface Temperature.

## 2.2. Data Sources

### 2.2.1. Observational and Reanalysis Data

Table 1 summarizes the observational and reanalysis datasets used in this study. The daily satellite SST data are from the National Oceanic and Atmospheric Administration (NOAA) Optimum Interpolation Sea Surface Temperature (OISST) High Resolution Dataset Version 2 (Reynolds et al., 2007). The daily SST anomalies are calculated relative to the climatology from 1983 to 2012. In addition, we also use the Hadley Centre Sea Ice and Sea Surface Temperature (HadISST) version 1 data (Rayner et al., 2003) and Centennial in situ Observation-Based Estimates (COBE) SST version 2 data (Hirahara et al., 2014) to compare the linear trend with OISST.

ERA5 is the fifth-generation global atmospheric reanalysis data from the European Centre for Medium-Range Weather Forecasts (ECMWF). The data from 1979 to present provide hourly estimates of a large number of variables for the atmosphere, land, and ocean. We use ERA5 to investigate the possible physical drivers of MHWs in this study. Figures S2 and S3 show that the daily SST of ERA5 is typically less than 1°C higher than OISST, which results in higher criteria of MHWs compared with those for OISST. However, ERA5 generally captures the spatiotemporal characteristics of the MHWs in the study area.

We use the China Ocean Reanalysis (CORA v1.0) products to investigate ocean surface currents in the Northwest Pacific Ocean, especially the role of the Kuroshio in MHWs. The available variables include sea surface height, SST, salinity, and ocean current information. Thirty-five layers are included in the vertical direction, and the monthly data cover the period from January 1958 to December 2017.

### 2.2.2. Global Climate Model Data

The daily outputs of SST from 28 global climate models (GCMs) from the Coupled Model Intercomparison Project Phase 5 (CMIP5) data archive are used to make future projections. Based on the evaluation of the annual and seasonal SST linear trend values, 12 climate models (Table 2) were selected with values between the three observation datasets and the ensemble mean of 28 climate models (Figure S4). The historical simulations for the twentieth century (1979–2005) and three Representative Concentration Pathway (RCP) projections for the 21st century (2006–2100), including the RCP2.6 (very low forcing level), RCP4.5 (low and middle forcing level), and RCP8.5 (very high forcing level) emission scenarios, were conducted (Taylor et al., 2012; Table S1). Due to the different spatial resolutions in GCMs, the data from the 12 models are interpolated to 0.5° × 0.5° grid resolution. To reduce the uncertainty in the results from different CMIP5 models, the multi-model ensemble mean with equal weight method is used.

## 2.3. Methods

### 2.3.1. Definition of MHWs

In this study, we use the definition of MHWs by Hobday et al. (2016) to identify MHWs and quantify MHWs from daily temperature measurements. A MHW is defined as a “discrete prolonged anomalously warm-water event at a particular location.” Specifically, “discrete” implies that the MHW is an identifiable event with a clear start and end dates, “prolonged” means that it has a duration of at least five days,

**Table 2***Horizontal Resolution (Longitude × Latitude) of the 12 CMIP5 Models Used in the Present Study*

Model name	Institution (country)	Ocean resolution
ACCESS1.0	Commonwealth Scientific and Industrial Research Organization (CSIRO) and Bureau of Meteorology (BoM; Australia)	360×300
ACCESS1.3	CSIRO and BoM (Australia)	360×300
CanESM2	Canadian Centre for Climate Modeling and Analysis (Canada)	256×19
CMCC-CM	Centro Euro-Mediterraneo per I Cambiamenti Climatici (Italy)	182×149
CMCC-CMS	Centro Euro-Mediterraneo per I Cambiamenti Climatici (Italy)	182×149
FGOALS-S2	Institute of Atmospheric Physics, Chinese Academy of Science (China)	360×196
GFDL-ESM 2M	Geophysical Fluid Dynamics Laboratory (USA)	360×200
HadGEM2-ES	Met Office Hadley Centre (UK)	360×216
IPSL-CM5A-MR	Institut Pierre-Simon Laplace (France)	182×149
IPSL-CM5B-LR	Institut Pierre-Simon Laplace (France)	182×149
MPI-ESM-LR	Max Planck Institute for Meteorology (MPI-M; Germany)	256×220
MPI-ESM-MR	Max Planck Institute for Meteorology (MPI-M; Germany)	802×404

and “anomalously warm” means the temperature is above a climatological threshold. Quantitatively, MHW events can be found by identifying periods when the daily SST is above the 90th percentile (threshold) of its seasonal variations for at least five consecutive days; two successive events separated by a 2-day or shorter break are considered as a single event. According to the processing method in Hobday et al., 2016, the 90th percentile was calculated for each calendar day using daily SSTs within an 11-day window centered on the data across all years within the climatology period, and smoothed by applying a 31-day moving average. The climatological mean and threshold for the NOAA OISST and 12 CMIP5 model data are calculated over a base period of 1983–2012.

### 2.3.2. Parameters Used for Describing MHWs

Based on previous studies (Hobday et al., 2016; Oliver et al., 2017, 2018), the parameters used to describe the characteristics of a MHW included the duration (i.e., the time period between the start and end dates) and mean intensity (i.e., the average temperature anomaly divided by the duration of the event) in this study, and the parameters regarding the statistical characteristics of the annual MHWs included the total days (i.e., the sum of days with MHW events per year), annual average duration (i.e., the average duration of MHWs per year), frequency (i.e., the number of MHW events per year), and annual mean intensity (the average mean intensity of MHWs per year). The software used for calculating the aforementioned parameters is available at [https://github.com/ZijieZhaoMMHW/m\\_mhw1.0](https://github.com/ZijieZhaoMMHW/m_mhw1.0).

In addition, linear trend analysis, the Mann-Kendall test, and Oceanic Niño Index (ONI), which tracks the running 3-month average SST in the Niño 3.4 region (the east-central tropical Pacific between 120 and 170°W), were also used.

## 3. Results

### 3.1. MHWs in the CMSOW During 1982–2018

Figure 1 shows the average and linear trends of the annual total days, duration, frequency, and mean intensity of MHWs from 1982 to 2018 relative to the 30-year climatology (1983–2012). The mean annual total days of MHW range from 14 to 39 days throughout the CMSOW, and higher-value areas are located in the coastal regions of the Bohai Sea, west of the Japan Sea, Beibu bay in the South China Sea, and east of the Taiwan Island (Figure 1a). The MHW annual total days show a linear increase of –5–30 days per decade during 1982–2018 ( $p < 0.01$ ; Figure 1e). The spatial distribution of the annual mean MHW duration is similar to that of the mean annual total days except in the South China Sea, where the higher-value area is closer to the lower-latitude direction. The fastest linear increase of the duration is 5–9 days per decade in the east of the Philippines and the South China Sea ( $p < 0.01$ ; Figures 1b and 1f).

The annual mean MHW frequency ranges from 1.5 to 3.4 per year (Figure 1c), with values higher than 3 in the East China Sea and north of the South China Sea. The MHW frequency also increases by 1–2 per decade during 1982–2018 ( $p < 0.01$ ; Figure 1g). The high annual mean total days in the northern South China Sea mainly result from the high frequency of MHWs, while those in the Bohai Sea result from a longer duration. In general, the annual mean intensity of MHWs increases northward (Figures 1d and 1h). The higher value

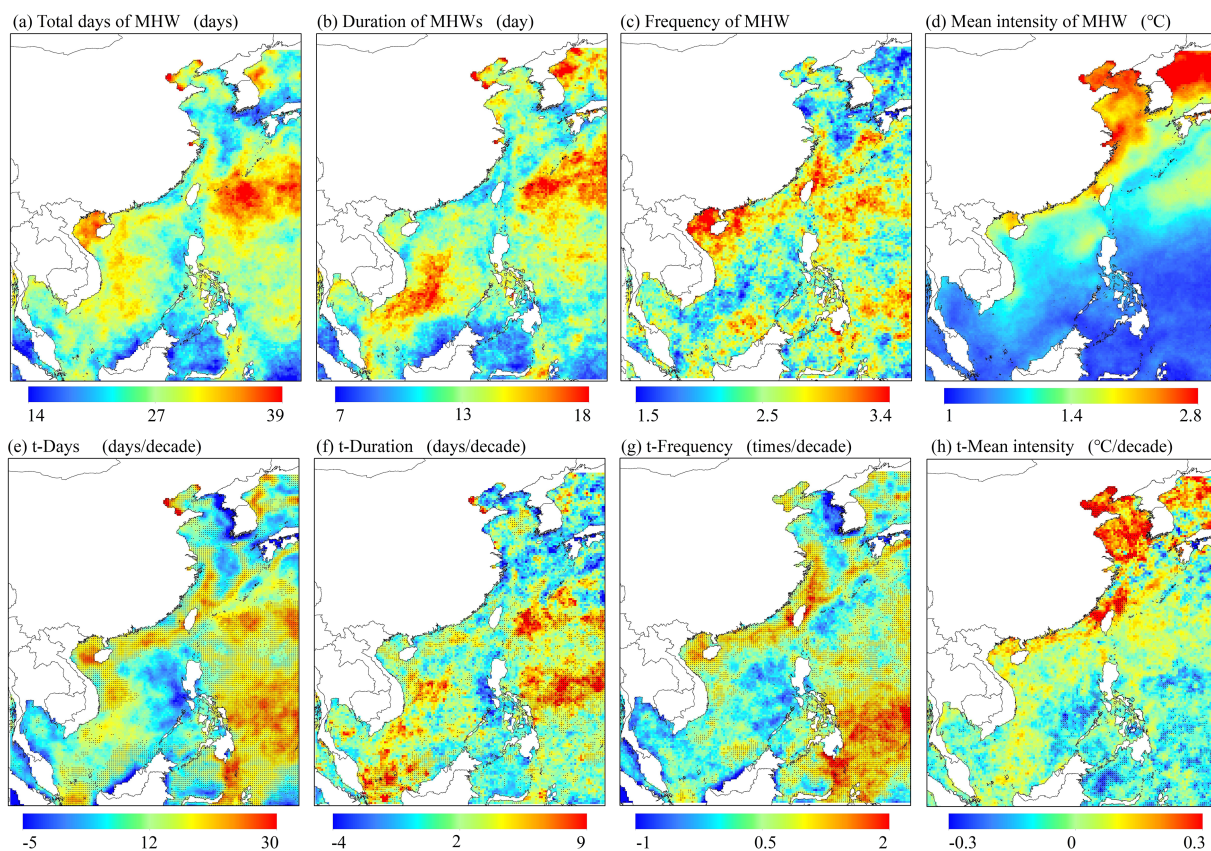


**Figure 1.** Characteristics of the marine heatwaves in China's marginal seas and adjacent offshore waters. The annual average marine heatwaves during 1982–2018: (a) total days, (b) duration, (c) frequency, and (d) mean intensity; the linear trend of the marine heatwaves during 1982–2018 per decade: (e) total days, (f) duration, (g) frequency, and (h) mean intensity. The dots indicate the located grids with a confidence level  $>99\%$ .

areas of mean intensity concentrate in the Bohai Sea, the Yellow Sea, west of East China Sea, and Japan Sea with values of 2–2.8°C and increasing rates at 0.1–0.3°C per decade ( $p < 0.01$ ) during 1982–2018.

Figure 2 shows the total days of MHW during summer (i.e., from June to September) and the line chart summarizes the number of the grids with MHW events per year and the ONI. The areas with MHWs are small and patchy before 2000, with total days less than 40 days (except for 1998). However, both the areas with MHWs and total days increase greatly after 2000, and the highest value of total days even exceeds 100 days. In general, the areas with MHWs in summer show increasing trends from 1982 to 2018 ( $R=0.47$ ,  $p < 0.01$ ) and are particularly large in strong El Niño years (e.g., 1998, 2014, and 2015).

### 3.2. MHWs in the Bohai Sea During 1982–2018

The Bohai Sea experiences severe MHWs in the CMSOW (Figure 1). Thus, three representative sites in the Liaodong, Bohai, and Laizhou Bays are selected to analyze the temporal variations in the local MHWs

**Table 3**  
*Contrast With the Global Average Linear Trend in Frequency, Duration, and Mean Intensity*

MHW parameters	Global	Study area	Bohai Sea	Three bays
Frequency (times/decade)	0.45	0.84	0.98 (117.8%)	1.02 (126.6%)
Mean intensity (°C/decade)	0.085	-0.01	0.15 (76.5%)	0.21 (148.2%)
Duration (days/decade)	1.3	1.72	1.28 (-1.6%)	2.87 (120.8%)
Sources	Oliver et al. (2018)	This study	This study	This study

*Note.* The values in the bracket indicate the growth rate relative to the global average linear trend.

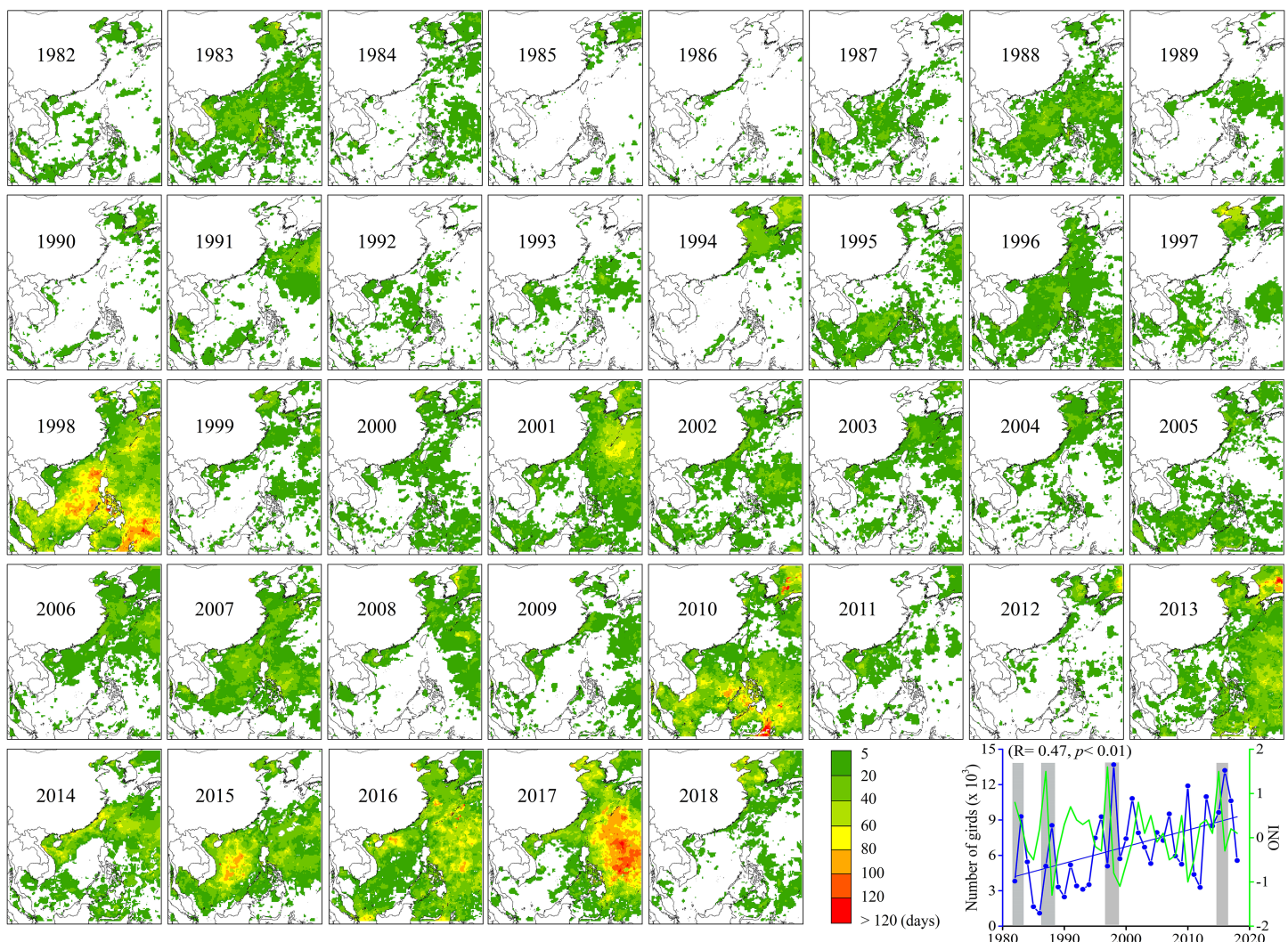


**Figure 2.** Total days of marine heatwaves; start day occurs from June to September, from 1982 to 2018. The line chart in the lower right corner counts the total number of grid points where marine heatwaves occur during June–September of each year (blue line) and Oceanic Niño Index value (green line). The gray shading area means periods of strong El Niño years.

(Figure 3). From June 2015 to September 2018, MHWs occur across all the three bays, especially between April and September in 2017 (Figures 3a–3c). As shown in Figure 2, the total days of MHW in 2017 are anomalously high, which can be attributed to the early start and long-lasting MHWs. The time series of SST shows that August 2018 is warmer than recent years, and the SST even exceeds  $30^{\circ}\text{C}$  for a few days. The SST anomalies (SSTA) in the three bays increase from 1982 to 2018 (relative to the 1983–2012 baseline climatology), and the amplitude of SSTA increases obviously after 2007, indicating that the increasing frequencies of MHWs may be caused by both long-term trend and natural variability (Figures 3d–3f).

Figure 4 shows the submarine contour line of the Bohai Sea and annual average total days, duration, frequency, and mean intensity of MHWs from 1982 to 2018. The highest values of the MHW's total days, duration, and mean intensity are all located in three shallow bays with depths of only 10–20 m, while the highest intensity is oppositely located in deeper areas. At the same time, most of the marine ranching facilities that have been and will be built are concentrated in shallow areas.

### 3.3. Characteristics of Future MHWs

With the increases in the intensity, frequency, and duration of MHW in the CMSOW over the past 37 years, it is very important to better understand the future trends of MHW under the combined effects of natural climate variability and anthropogenic climate change.

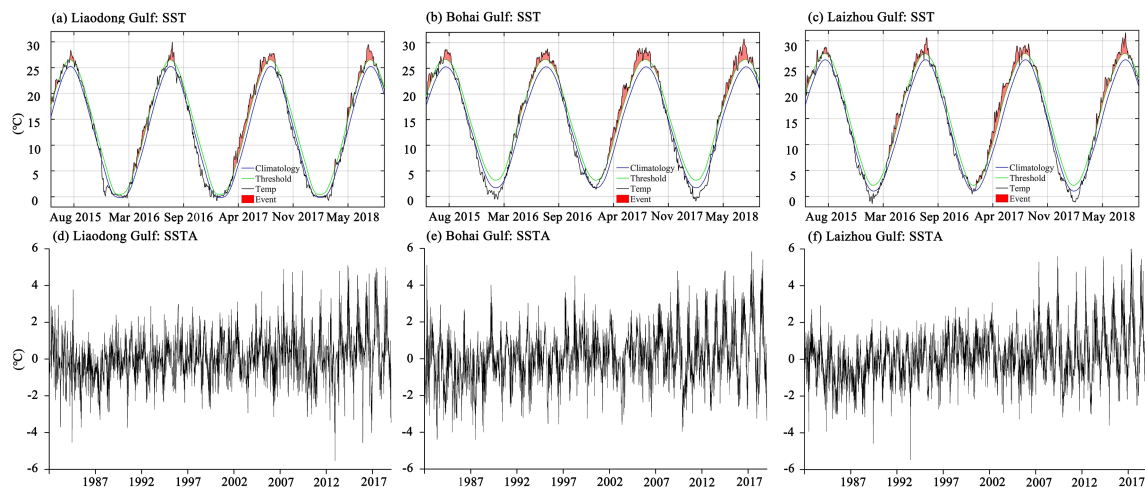


**Figure 3.** (a–c) Domain daily averaged sea surface temperature (SST; upper plots) and (d–f) SST anomalies (bottom plots) in Liaodong, Bohai, and Laizhou Bay from National Oceanic and Atmospheric Administration (NOAA) Optimum Interpolation Sea Surface Temperature (OISST) V2. In the upper plots, the curves correspond to the SST (black), the 90th percentile seasonally varying threshold (green), and the climatology (blue). The red shaded regions indicate marine heatwaves. The time span in upper plots is from June 2015 to September 2018 and in bottom plots is 1982 to 2018.

The areas with higher total days and duration will increase from RCP2.6 to 8.5 scenarios. In RCP 2.6, the total days in the CMAOW are less than 150 days; in most of the study areas, however, the total days are over 200 and 250 days in RCP4.5 and 8.5, respectively (Figures 5a and 5b, 5e and 5f, and 5i and 5j). The duration of

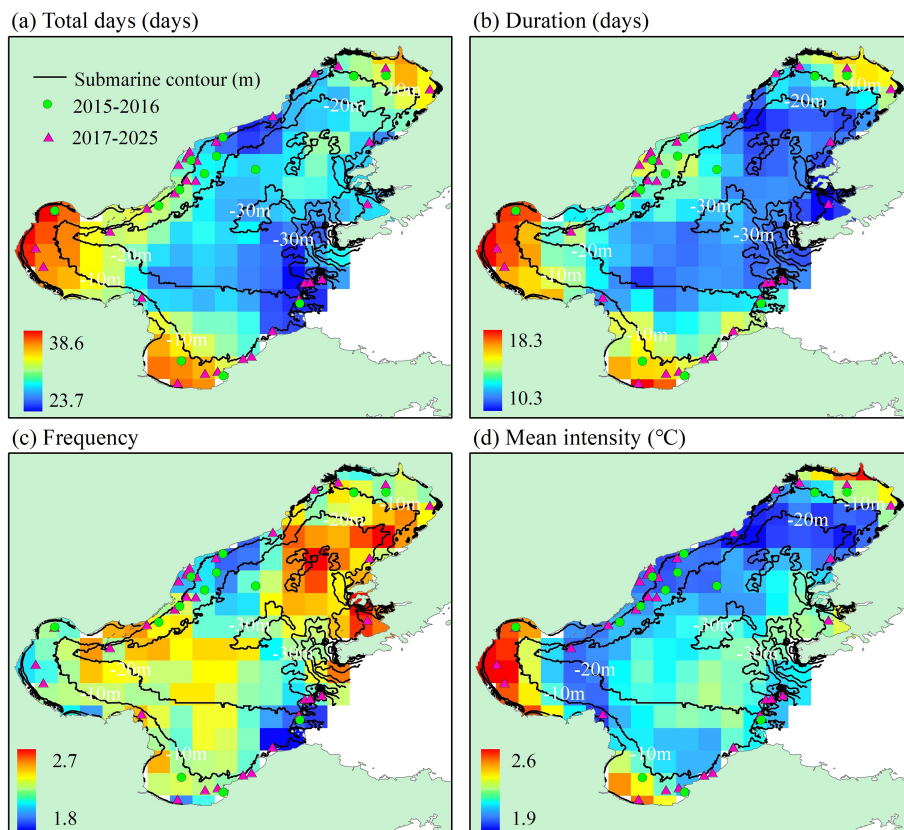


**Figure 4.** The Bohai Sea bathymetry and average metrics of marine heatwaves from 1982 to 2018. (a) Total days, (b) duration, (c) frequency, and (d) mean intensity. Circles and triangles represent marine ranching built in 2015–2016 and 2017–2025, respectively.

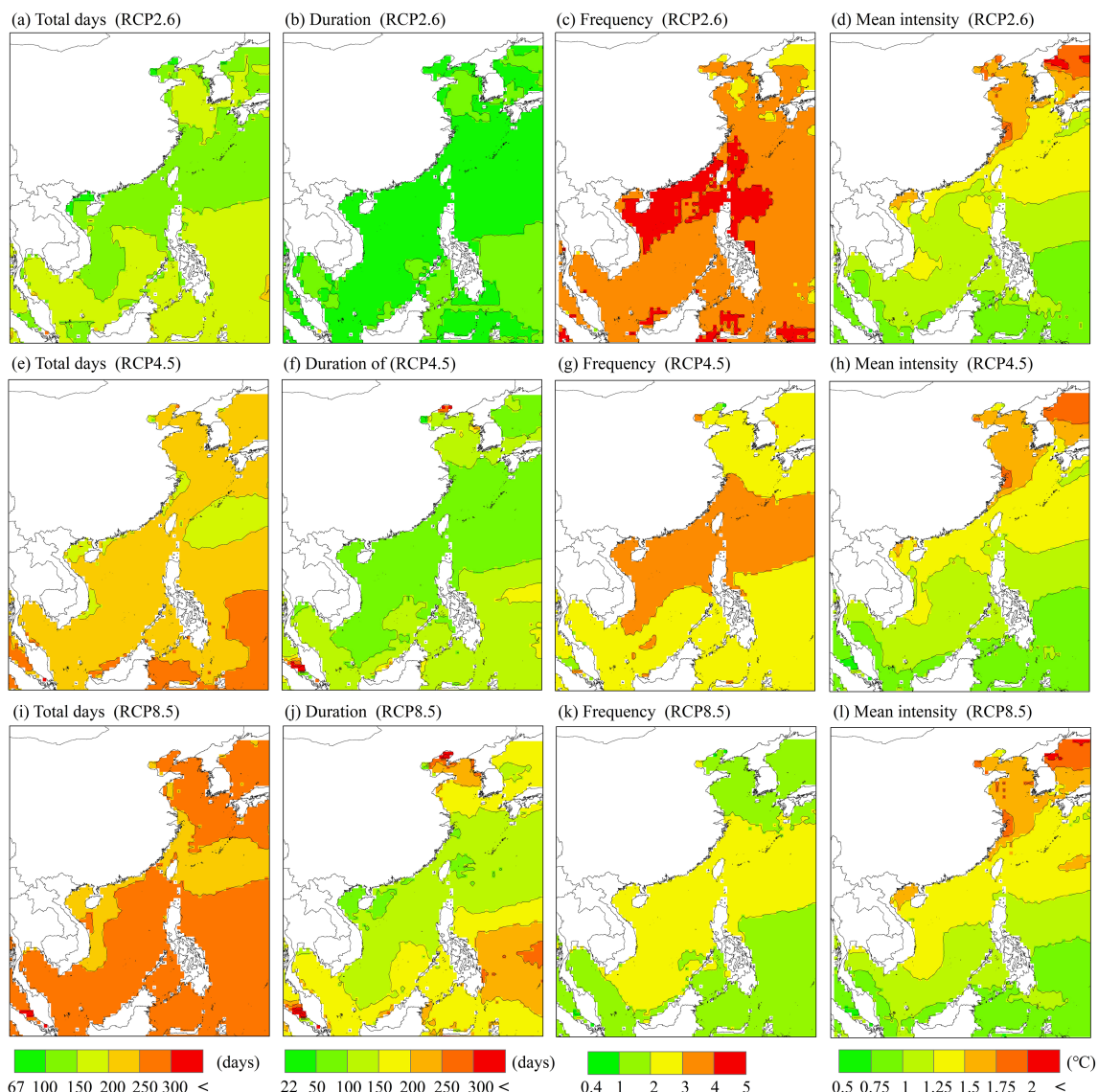


**Figure 5.** The future spatial patterns of marine heatwaves under three Representative Concentration Pathways by the multimodel ensemble mean method (2006–2100). (a, e, and i) average total days, (b, f, and j) average duration, (c, g, and k) average frequency, and (d, h, and l) average mean intensity.

MHWs will increase from less than 50 days in RCP2.6 to about 200 days in RCP8.5. It is worth noting that the Bohai Sea and the Yellow Sea are the regions with the longest duration of MHWs in China under RCP4.5 and RCP8.5 scenarios, reaching 250 days or more (Figure 5j). Under RCP8.5, the frequency is reduced from the highest 4–5 in the northern part of the South China Sea under RCP2.6 to the 1–2 in the northern and southern parts of the study area, and 2–3 in the central area (Figures 5c, 5j, and 5k). This is because the spatial patterns of mean MHW duration and frequency have a negative relationship (Oliver et al., 2018). The spatial pattern of mean intensity does not change much in the three RCPs, and the higher-value areas are mainly concentrated in the Bohai Sea, the Yellow Sea, north of East China Sea, and Japan Sea, ranging from 1.75 to 2°C (Figures 5d, 5h, and 5l). In summary, from the perspective of spatial pattern, the areas with higher total days and duration will increase; frequency has a negative spatial pattern relationship with duration; the spatial pattern of mean intensity is mostly unchanged.

Variations in the total days of MHWs show an increasing trend from 1982 to 2100, and the range is up to 150 days in RCP2.6, 300 days in RCP4.5, and 350 days in RCP8.5, respectively (Figure 6a). Time series of the duration also show an increase trend range from 50 days to 150 and 250 days in RCP4.5 and 8.5,

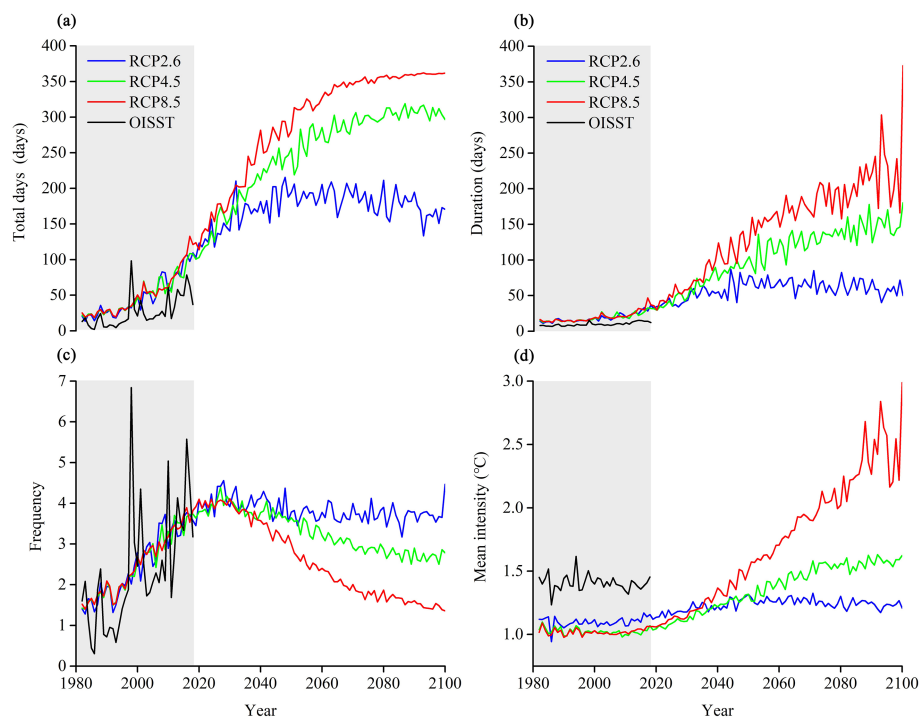


**Figure 6.** Time series of an annual mean of marine heatwaves under Representative Concentration Pathways (RCPs) 2.6 (blue line), 4.5 (green line), and 8.5 (red line) from 1982 to 2100 based on the multimodel ensemble mean method. (a) Total days, (b) duration, (c) frequency, and (d) mean intensity of marine heatwaves. The gray shading means periods of 1982–2018. The black line means corresponding Optimum Interpolation Sea Surface Temperature (OISST) result during 1982–2018.

respectively (Figure 6b). There is a clear opposite trend in the frequency, that is, increasing rapidly from 1982 to 2030, reaching a peak value of 4, and then starting to decrease (Figure 6c). Variation of mean intensity increases slowly between RCP2.6 and 4.5, less than 1.5°C; but for RCP8.5, the value increases fast after 2040 and reaches the maximum of nearly 2.5–3°C (Figure 6d). Compared with the OISST results in past and current, the multimodel ensemble mean overestimated total days and duration but underestimated mean intensity, and only frequencies are consistent. The MHW values simulated by GCMs last longer and have a wider distribution than the observed ones, which is probably due to the relatively coarse resolution of the GCMs (Frölicher et al., 2018). For the perspective of temporal variation, 2040 is a key node for the future changes of MHW under different RCPs. For example, the increasing trend of total days changes from fast to slow, and frequency shows an opposite trend; the duration and mean intensity rise faster after 2040.

## 4. Discussion

### 4.1. Comparison of the MHWs in the CMSOW and Globe

The spatial patterns of the MHW duration and frequency are found to be consistent with observed secular patterns of SST warming during 1982–2018 (Figure 7, Table 3). We use COBE2, HadISST1, and OISST to calculate the observed secular SST trend in summer (June–July–August) and winter (December–January–February). Both the SST linear trends from HadISST1 and OISST show the most rapid increase in the coastal Bohai Sea and west of the Yellow Sea and Japan Sea, at a rate of up to 0.2–0.3°C per decade in summer (Figures 7a–7c). In winter, the three SST data sets show that the East China Sea is the fastest warming region, with a warming rate of 0.3–0.4°C per decade (Cai et al., 2017). We found that HadISST1 and OISST also show a faster SST warming in most parts of the Bohai Sea and the Yellow Sea, and west of Japan Sea similar to summer warming (Figures 7c–7e).

The spatial distribution of the increase in the SST is synchronized with the ocean warming in CMSOW, especially in shallow areas (Hoegh-Guldberg et al., 2014). However, the warming rate of SST in the

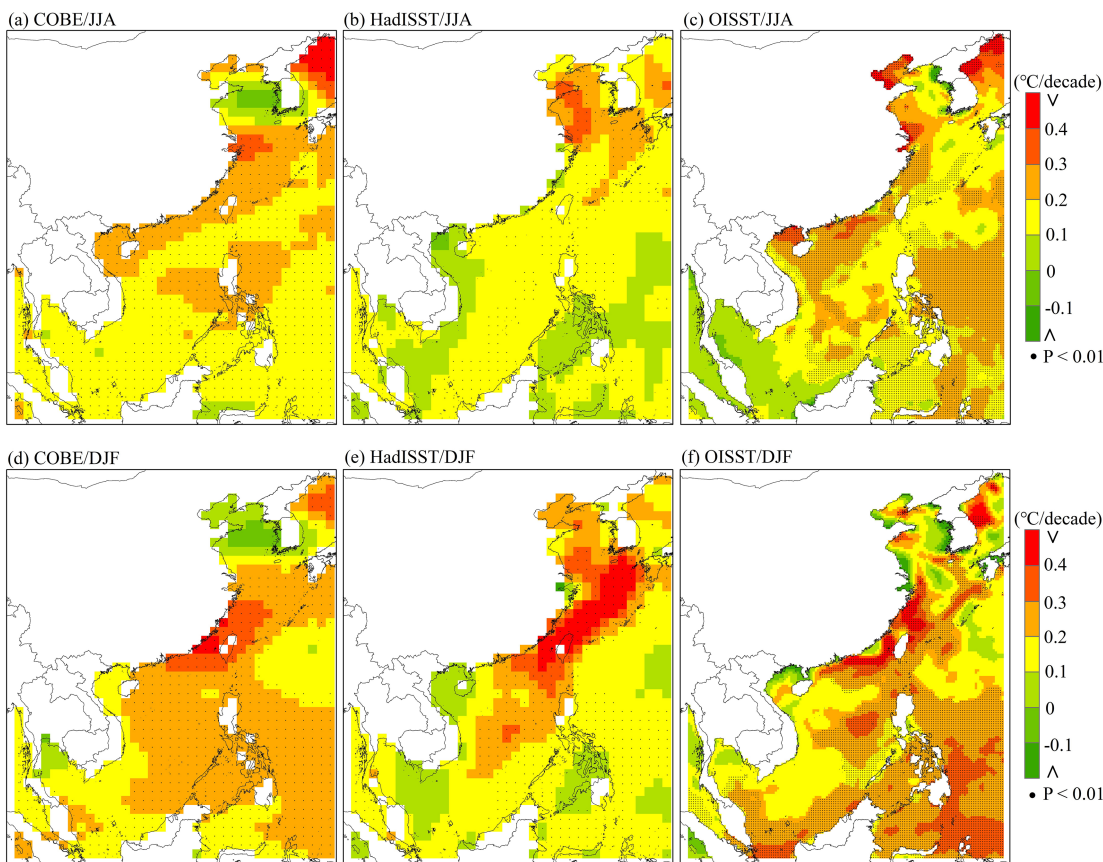


**Figure 7.** Sea surface temperature linear trends during the (a–c) summers and (d–f) winters based on theennial in situ Observation-Based Estimates sea surface temperature version 2 (COBE-SST2; 1979–2017), Hadley Centre Sea Ice and Sea Surface Temperature version 1 (HadISST1; 1979–2017), and Optimum Interpolation Sea Surface Temperature (OISST; 1982–2017) datasets, respectively. The dots indicate the located grids with a confidence level  $>99\%$ .

CMSOW is higher than the global mean warming rate of  $0.2^{\circ}\text{C}$  per decade (Rhein et al., 2013). The robust surface warming in offshore China since the 1980s is partly due to the weakening East Asia monsoon and increasing warmth of the Kuroshio Current (Cai et al., 2017; Tang et al., 2009; Wu et al., 2012). We also found that in the CMSOW, the shallow and semienclosed Bohai Sea experiences severe MHWs (Figure 1) and robust warming trend in both summer and winter (Figure 7). The values of the linear trend of frequency and duration in the Bohai Sea increase by 117.8% and 76.5%, respectively, when compared with study by Oliver et al. (2018); zoomed to the three bays in the Bohai Sea, all MHW characteristics increase at least 120% than the globe. In summary, robust sea surface warming can largely explain the occurrence of MHW; regions with a faster SST warming rate, especially in coastal zones, are more conducive to suffer severe MHW.

#### 4.2. Driving Mechanisms

Long-term ocean warming can be caused by air-sea heat flux and variations in ocean circulation (Oliver et al., 2017). The heat transfer across the air-sea boundary plays a crucial role in the atmospheric and oceanic circulation (Moore et al., 2012). The ERA5 daily heat flux data have been used to document the characteristics of the anomalous air-sea heat fluxes from June to September of 2017 when more and longer MHWs occur (Figure 3). Figures 8a–8d show that the MHWs generally occur in positive net heat flux areas, which indicate heat gain by the ocean (Benthuyzen et al., 2018). The associated decrease in cloud cover increases solar shortwave radiation at the ocean's surface (McCabe et al., 2016; Figures 8e–8h). Latent heat loss from the ocean to the atmosphere (evaporative cooling) decreases (positive anomalies in Figures 8i–8l) due to the effect of weak winds. We also pick out four points with longer consecutive MHW days and higher frequency near the coast oceans (Geolocation shows in Figure 8a). Figures S5–S8 reveal that changes in solar shortwave

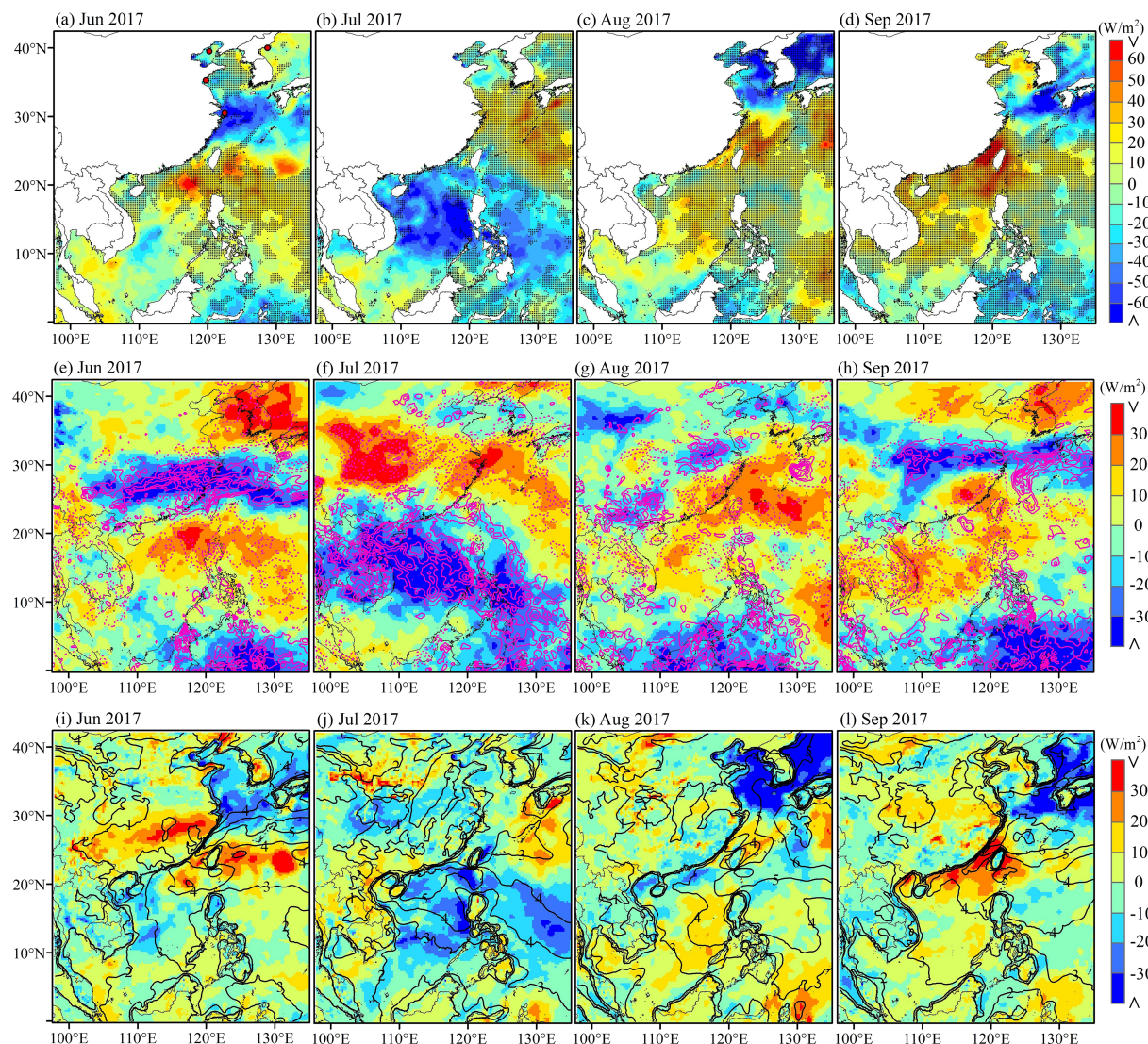


**Figure 8.** Composites of anomalies (1982–2018). (a–d) Net heat flux (i.e., surface net solar radiation minus the total of surface net thermal radiation, latent heat flux, and sensible heat flux) anomalies from June to September 2017; the black dots represent the occurrence of marine heatwaves. (e–h) Surface net solar radiation (color shading in the figures) and total precipitation anomalies (the solid pink line means positive value; the dashed pink line means negative value). (i–l) Latent heat flux (color shading) and 10-m wind speed (m/s) anomalies (black line).

radiation generate the largest changes before September. In winter, a cyclone that approaches from the northwest will bring cooler and drier air to the MHW area and drastically enhances the evaporative cooling. As a consequence, the MHW event comes to end. The increased solar shortwave radiation due to reduced cloud cover and reduced ocean heat loss from weaker winds are the main contributors to the MHW occurrences in the region (Benthuyzen et al., 2018; Rodrigues et al., 2019). Moreover, weaker coastal winds reduce wind stress, leading to weakened coastal upwelling, which results in a rise in SST (Robinson, 2016). Other components of heat flux, longwave thermal radiation, and sensible heat flux are of lesser importance.

The Kuroshio Current plays an important role in causing SST anomalies of the northwest Pacific Ocean (Hu et al., 2015; Kelly et al., 2010; Kwon et al., 2010). Oliver et al. (2018) found that mean MHW intensity increased by over 65% of the global ocean between 1982–1998 and 2000–2016 and most notably in the WBC regions, where the background warming has been faster than the global average. Figures S9a–S9g show the mean ocean current velocity anomaly at 10 m from June to September. The results show a weakening Kuroshio by 2 cm per year during the period ( $p < 0.01$ ); Kuroshio also decreased by up to 0.5 m/s in

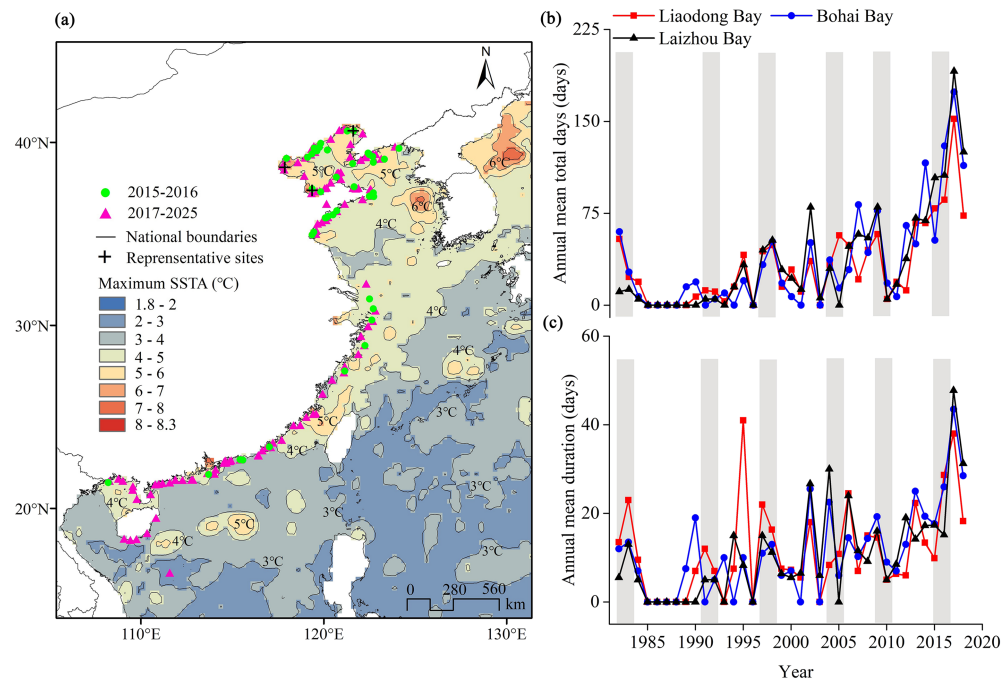


**Figure 9.** (a) Maximum sea surface temperature anomalies and the locations of marine ranching. The green dot represents the national marine ranching demonstration zones that have been built from 2015 to 2016; the pink triangle represents the planned national marine ranching demonstration zones in 2017–2025. The line chart on the right shows (b) the annual mean total days and (c) the duration of marine heatwaves. The red line stands for Liaodong bay, the blue line stands for Bohai bay, and the black line stands for Laizhou bay. The gray shading represents the periods of El Niño years.

strong El Niño years, especially in 2013 and 2014. Wang et al. (2016) also found a weakened Kuroshio during 1993–2013 based on five datasets, and a weaker but warmer Kuroshio capable of redistribute mass and energy between the marginal seas and Pacific by conveying less heat to the South China Sea but more heat to the East China Sea, from the warming western North Pacific warm pool.

The interannual variability of SST is linked with El Niño–Southern Oscillation (ENSO) teleconnection, through which anomalous surface heat flux warms or cools the Eastern marginal seas of China during El Niño or La Niña events (Wu et al., 2017). Cheng et al. (2019) confirmed that high SST will drive more air-sea heat fluxes into the atmosphere during El Niño, resulting in a strong negative ocean heat content tendency in the tropical Pacific Ocean. Several MHWs were primarily driven by large-scale El Niño events that affected ocean climate at large spatial scales (Smale et al., 2019). Yin et al. (2018) found a big jump of record warm global mean surface temperature over the 2014–2016 as a consequence of an El Niño releasing large amounts of ocean heat from the northwestern tropical Pacific. Our result also shows that the MHWs in 1998, 2015, and 2016 are outstanding due to the strong El Niño events (Figure 2).

In addition, increasing anthropogenic influences, persist extremely high air temperature, atmospheric block are probably led to an intense MHWs (Manta et al., 2018; Oliver et al., 2017, 2018); ocean bathymetry also has a great impact on the distribution of MHWs, such as shallow, semiclosed Bohai Sea.

#### 4.3. Potential Ecological Impacts

##### 4.3.1. Negative Impacts on Fishery Resources

The construction of marine ranching is prevalent in China's marginal seas recently (Yang et al., 2019), and most marine ranching is built in shallow waters with depths of 6–20 m near the coastal area (Yang et al., 2016; Yang et al., 2019). The Bohai Sea and the Yellow Sea are the key habitats for sea cucumber (Yang et al., 2019). We found that the maximum SSTA values in three bays of the Bohai Sea are generally higher than 5°C, or even 8°C in the nearshore area; the maximum SSTA values in the Yangtze River estuary and Hangzhou bay are over 4°C (Figure 9a). The variation of annual mean total days and frequency of MHWs in three representative sites show increasing trends, especially between 2010 and 2018 (Figures 9b and 9c). Under global climate change, the marine ranching is facing various risks and even large-scale seasonal

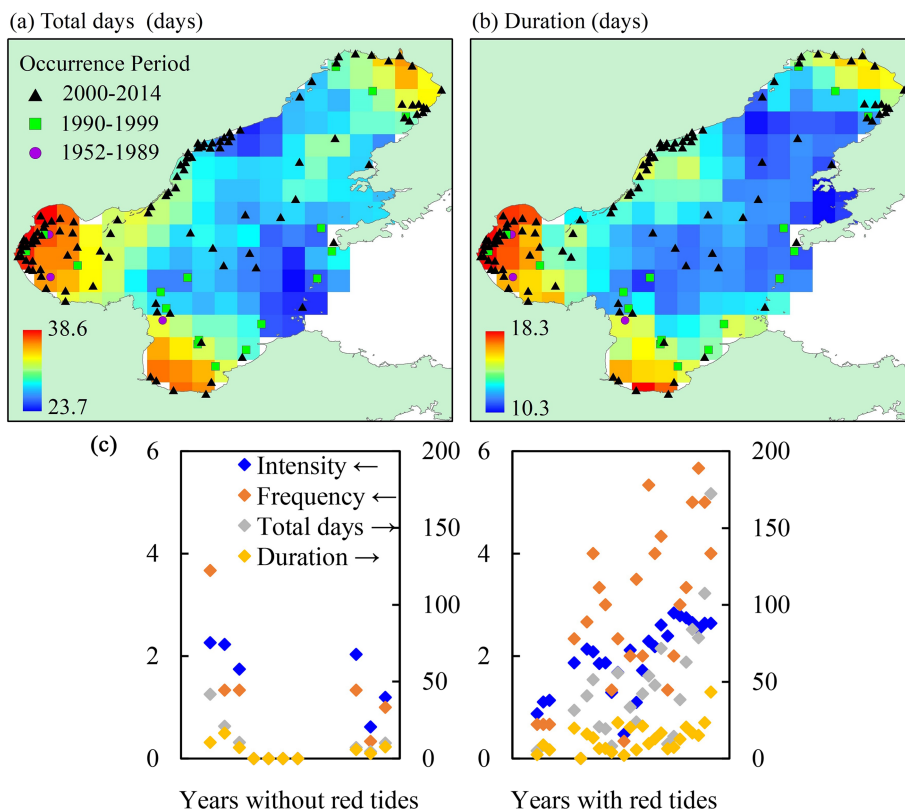


**Figure 10.** (a) Average total days and (b) duration of marine heatwaves in the Bohai Sea overlay with the harmful algal blooms. Harmful algal bloom data were obtained from Song et al., 2016. (c) The temporal changes of total days (days), duration (days), frequency, and mean intensity ( $^{\circ}\text{C}$ ) in the years with and without red tide occurrences in the Bohai Sea during 1982–2018. The red tides data in the Bohai Sea were obtained from the China Marine Statistical Yearbook and State Oceanic Administration, People's Republic of China, Chinese Marine Disaster Bulletins.

biological death due to high temperature and low DO (Hu et al., 2019a, 2019b; Liu et al., 2014; Yang et al., 2019). Climate models predict declines in oceanic DO produced by global warming, and reduced oxygen levels (Breitburg et al., 2018; Schmidtko et al., 2017; Stramma et al., 2008). In August 2011, a significant decrease in the DO in the bottom layer (at 20- to 35-m depth) in the northwestern and northern parts of the Bohai Sea was found (Zhai et al., 2012). In August 2014, two oxygen-deficient zones in the Bohai Sea were observed, where the second largest oxygen-deficient zone in China's marginal seas is found (Zhao et al., 2017). It is worth noting that most of the marine ranching zones in the Bohai Sea are also distributed in these shallow bays and coastal areas. Therefore, the flora and fauna in these marine ranching ecosystems could be severely impacted by the frequent, long-lasting, and strong MHWs.

#### 4.3.2. Potential Impacts on Harmful Algae Blooms (HABs)

Previous studies showed that increasing ocean temperature is an important factor facilitating the intensification of HABs in coastal waters (Cavole et al., 2016; Gobler et al., 2017; McCabe et al., 2016; Wells et al., 2015; Zhu et al., 2017). HABs have increased in frequency and spatial extent globally (Song et al., 2016) and could exert negative effects on aquatic ecosystems, fisheries, tourism, and human health (Gobler et al., 2017). As the annual mean total days and duration of MHWs in the Bohai Sea increased during the past four decades (Figures 9b and 9c), the HAB occurrences during the 2000–2014 period are much more frequent than during the 1990–1999 and 1952–1989 period (Figures 10a and 10b). Since 1880, the 10 warmest years in the instrumental record, except 1998, have now occurred after 2000 (Climate Central, 2019). The red tides occurred in the Bohai Sea during the same period were also obtained to analyze their relationship with four indexes of the MHWs from the mean of three representative sites (Figure 9a). The MHW total days or frequency tended to be higher in years with red tide occurrences than in years without red tide occurrences (Figure 10c). Besides, the spatial distribution of the HABs in the Bohai Sea also showed that the occurrences of red tides tend to concentrate in the three bays of the Bohai Sea, where the total days

and duration of MHWs are also higher than that in adjacent waters (Figures 10a and 10b). Considering the HABs have the same spatiotemporal characteristics with MHWs in the Bohai Sea, it is necessary to determine whether HABs would become more prevalent with warming coastal seas in the future.

The significant increases in MHW's total days and duration from 1982 to 2100 will probably increase the risk of severe, pervasive, and long-lasting impact on marine organisms (Smale et al., 2019). Importantly, these trends can largely be explained by increases in ocean surface warming; we can expect a continued global increase in MHW's total days and duration in the future with major impacts on fisheries, aquaculture, and tourism (Caputi et al., 2016; Hughes et al., 2017; Mills et al., 2013; Oliver et al., 2018). Given the likelihood of projections of intensifying extreme warming events with anthropogenic climate change (Coulomou & Rahmstorf, 2012), marine conservation and management approaches must consider MHWs and other extreme climatic events if they are to maintain and conserve the integrity of marine ecosystems under continued global warming, especially in shallow marginal seas.

## 5. Conclusions

In this study, the past, current, and future MHWs in the CMSOW were estimated from the daily OISST and 12 CMIP5 models. The potential ecological impacts of MHWs and possible driving mechanisms are discussed. The major conclusions of the study are as follows.

1. The Bohai Sea, Japan Sea, Beibu Bay, and east of Taiwan Island have the highest mean annual total days. The linear trend shows 20–30 days per decade increase in these regions ( $p < 0.01$ ). The linear trend of MHW duration in the east of Taiwan Island and the South China Sea is 5–9 days per decade ( $p < 0.01$ ). The East China Sea and north of the South China Sea have the most frequent MHWs (more than 3 times) and show a linear increase of 1–2 per decade ( $p < 0.01$ ). The mean intensity is higher in the north of the study area with a linear trend of 0.1–0.3°C per decade ( $p < 0.01$ ).
2. The Bohai Sea experiences severe MHWs in the CMSOW. The MHW frequency, duration, and mean intensity in its three bays double those of global average, which could negatively impact on fishery resources and increase HABs locally. Bathymetry is an important factor for MHWs in this region.
3. From the perspective of spatial pattern, the areas with longer total days and duration are increasing; frequency has a negative spatial pattern relationship with duration; the spatial pattern of mean intensity is mostly unchanged. From the perspective of temporal variation, 2040 is a key node for the future changes of MHW under different RCPs. For example, the trend of total days increases from fast to slow and that of frequency opposite; the duration and mean intensity rise faster after 2040.
4. The spatial patterns of MHW duration and frequency are consistent with observed patterns of SST warming. The increased solar radiation due to reduced cloud cover and reduced ocean heat loss from weaker wind speed are the main contributors to MHWs. A weaker and warmer Kuroshio is capable of redistributing mass and energy between the marginal seas and the open Pacific with more heat delivered into the East China Sea. El Niño also has a significant effect on MHWs.

## References

- Benthuysen, J. A., Oliver, E. C., Feng, M., & Marshall, A. G. (2018). Extreme marine warming across tropical Australia during Austral summer 2015–2016. *Journal of Geophysical Research: Oceans*, 123, 1301–1326. <https://doi.org/10.1002/2017JC013326>
- Breitburg, D., Levin, L. A., Oschlies, A., Grégoire, M., Chavez, F. P., & Conley, D. J. (2018). Declining oxygen in the global ocean and coastal waters. *Science*, 359, 46.
- Cai, R. S., Tan, H. J., & Kontoyiannis, H. (2017). Robust surface warming in offshore China seas and its relationship to the East Asian Monsoon wind field and ocean forcing on inter-decadal timescales. *Journal of Climate*, 30(22), 8987–9005. <https://doi.org/10.1175/JCLI-D-16-0016.1>
- Caputi, N., Kangas, M., Denham, A., Feng, M., Pearce, A., Hetzel, Y., & Chandrapavan, A. (2016). Management adaptation of invertebrate fisheries to an extreme marine heat wave event at a global warming hot spot. *Ecology and Evolution*, 6(11), 3583–3593. <https://doi.org/10.1002/ece3.2137>
- Cavole, L. M., Demko, A. M., Diner, R. E., Giddings, A., Koester, I., Pagniello, C. M. L. S., et al. (2016). Biological impacts of the 2013–2015 warm-water anomaly in the Northeast Pacific: Winners, losers, and the future. *Oceanography*, 29(2), 273–285.
- Chen, K., Gawarkiewicz, G. G., Lentz, S. J., & Bane, J. M. (2014). Diagnosing the warming of the Northeastern US Coastal Ocean in 2012: A linkage between the atmospheric jet stream variability and ocean response. *Journal of Geophysical Research: Oceans*, 119, 218–227. <https://doi.org/10.1002/2013JC009393>
- Cheng, L. J., Trenberth, K. E., Fasullo, J. T., Mayer, M., Balmaseda, M., & Zhu, J. (2019). Evolution of ocean heat content related to ENSO. *Journal of Climate*, 32(12), 3529–3556. <https://doi.org/10.1175/JCLI-D-18-0607.1>
- Climate Central (2019). The 10 hottest global years on record. Retrieved from <https://www.climatecentral.org/gallery/graphics/the-10-hottest-global-years-on-record>

## Acknowledgments

This study was supported by the Natural Science Foundation of China (41471431), the Program B for Outstanding PhD candidate of Nanjing University (201902B074), the China Scholarship Council (201806190149), the Marine Science and Technology 508 Innovation Project of Jiangsu Province (HY2018-9), and the Fundamental Research 509 Funds for the Central Universities (grant 14380001). We thank Zijie Zhao for providing the main function code to detect marine heat-wave events ([https://github.com/ZijieZhaoMMHW/m\\_mhw1.0](https://github.com/ZijieZhaoMMHW/m_mhw1.0)). NOAA High Resolution SST V2 data and COBE-SST2 data provided by the NOAA/OAR/ESRL PSD, Boulder, Colorado, USA, from their Web site at <https://www.esrl.noaa.gov/psd/>. The Met Office Hadley Centre's sea ice and sea surface temperature (SST) data set (HadISST1) is available at <https://www.metoffice.gov.uk/hadobs/hadisst/>. The daily mean sea surface temperature data from 12 models are obtained from <http://esgf-node.llnl.gov/search/cmip5/>. ERA5 dataset is available at <https://www.ecmwf.int/en/forecasts/datasets/reanalysis-datasets/era5>. The ocean current velocity data support from National Marine Science Data Center, National Science and Technology Resource Sharing Service Platform of China (<http://mds.nmds.org.cn/>). The Oceanic Niño Index is downloading from [https://origin.cpc.ncep.noaa.gov/products/analysis\\_monitoring/ensostuff/ONI\\_v5.php](https://origin.cpc.ncep.noaa.gov/products/analysis_monitoring/ensostuff/ONI_v5.php).

- Coumou, D., & Rahmstorf, S. (2012). A decade of weather extremes. *Nature Climate Change*, 2, 494–496.
- Di Lorenzo, E., & Mantua, N. (2016). Multi-year persistence of the 2014/2015 North Pacific marine heatwave. *Nature Climate Change*, 6(11), 1042–1047. <https://doi.org/10.1038/nclimate3082>
- Feng, M., McPhaden, M. J., Xie, S. P., & Hafner, J. (2013). La Niña forces unprecedented Leeuwin Current warming in 2011. *Scientific Reports*, 3(1), 1277. <https://doi.org/10.1038/srep01277>
- Frölicher, T. L., Fischer, E. M., & Gruber, N. (2018). Marine heatwaves under global warming. *Nature*, 560(7718), 360–364. <https://doi.org/10.1038/s41586-018-0383-9>
- Garrabou, J., Coma, R., Bensoussan, N., Bally, M., Chevaldonnè, P., Cligliano, M., et al. (2009). Mass mortality in Northwestern Mediterranean rocky benthic communities: Effects of the 2003 heat wave. *Global Change Biology*, 15(5), 1090–1103. <https://doi.org/10.1111/j.1365-2486.2008.01823.x>
- Gobler, C. J., Doherty, O. M., Hattenrath-Lehmann, T. K., Griffith, A. W., Kang, Y., & Litaker, R. W. (2017). Ocean warming since 1982 has expanded the niche of toxic algal blooms in the North Atlantic and North Pacific oceans. *Proceedings of the National Academy of Sciences of the United States of America*, 114(19), 4975–4980. <https://doi.org/10.1073/pnas.1619575114>
- Han, G. J., Fu, H. L., Zhang, X. F., Li, W., Wu, X. R., Wang, X. D., & Zhang, L. (2013). A global ocean reanalysis product in the China Ocean Reanalysis (CORA) project. *Advances in Atmospheric Sciences*, 30(6), 1621–1631. <https://doi.org/10.1007/s00376-013-2198-9>
- Hersbach, H., de Rosnay, P., Bell, B., Schepers, D., Simmons, A., Soci, C., ... Berrisford, P. (2018). Operational global reanalysis: progress, future directions and synergies with NWP. Retrieved from <https://www.ecmwf.int/node/18765>
- Hirahara, S., Ishii, M., & Fukuda, Y. (2014). Centennial-scale sea surface temperature analysis and its uncertainty. *Journal of Climate*, 27(1), 57–75. <https://doi.org/10.1175/JCLI-D-12-00837>
- Hobday, A. J., Alexander, L. V., Perkins, S. E., Smale, D. A., Straub, S. C., Oliver, E. C., et al. (2016). A hierarchical approach to defining marine heatwaves. *Progress in Oceanography*, 141, 227–238. <https://doi.org/10.1016/j.pocean.2015.12.014>
- Hoegh-Guldberg, O., Cai, R. S., Poloczanska, E. S., Brewer, P. G., Sundby, S., Hilmi, K., et al. (2014). The Ocean. In V. R. Barros, et al. (Eds.), *Climate change 2014: Impacts, adaptation, and vulnerability. Part B: Regional aspects*, (pp. 1655–1731). Cambridge: Cambridge University Press.
- Holbrook, N. J., Scannel, H. A., Gupta, A. S., Benthuysen, J. A., Feng, M., Oliver, E. C. L., et al. (2019). A global assessment of marine heatwaves and their drivers. *Nature Communications*, 10(1), 2624. <https://doi.org/10.1038/s41467-019-10206-z>
- Hu, D. X., Wu, L. X., Cai, W. J., Gupta, A. S., Ganachaud, A., Qiu, B., et al. (2015). Pacific western boundary currents and their roles in climate. *Nature*, 522(7556), 299–308. <https://doi.org/10.1038/nature14504>
- Hughes, T. P., Kerry, J. T., Álvarez-Noriega, M., Álvarez-Romero, J. G., Anderson, K. D., Baird, A. H., et al. (2017). Global warming and recurrent mass bleaching of corals. *Nature*, 543(7645), 373–377. <https://doi.org/10.1038/nature21707>
- Huo, D., Sun, L. N., Zhang, L. B., Ru, X. S., Liu, S. L., & Yang, H. S. (2019a). Metabolome responses of the sea cucumber *Apostichopus japonicus* to multiple environmental stresses: Heat and hypoxia. *Marine Pollution Bulletin*, 138, 407–420. <https://doi.org/10.1016/j.marpolbul.2018.11.063>
- Huo, D., Sun, L. N., Zhang, L. B., Ru, X. S., Liu, S. L., Yang, X. Y., & Yang, H. (2019b). Global-warming-caused changes of temperature and oxygen alter the proteomic profile of sea cucumber *Apostichopus japonicas*. *Journal of Proteomics*, 193, 27–43. <https://doi.org/10.1016/j.jprot.2018.12.020>
- Jacob, M. G., Hazen, E. L., Zaba, K. D., Rudnick, D. L., Edwards, C. A., Moore, A. M., & Bograd, S. J. (2016). Impacts of the 2015–2016 El Niño on the California current system: Early assessment and comparison to past events. *Geophysical Research Letters*, 43, 7072–7080. <https://doi.org/10.1002/2016GL069716>
- Jones, T., Parrish, J. K., Peterson, W. T., Bjorkstedt, E. P., Bond, N. A., Ballance, L. T., et al. (2018). Massive mortality of a planktivorous seabird in response to a marine heatwave. *Geophysical Research Letters*, 45, 3193–3202. <https://doi.org/10.1002/2017GL076164>
- Kelly, K. A., Small, R. J., Samelson, R. M., Qiu, B., Joyce, T. M., Kwon, Y. O., & Cronin, M. F. (2010). Western boundary currents and frontal air-sea interaction: Gulf Stream and Kuroshio Extension. *Journal of Climate*, 23(21), 5644–5667. <https://doi.org/10.1175/2010JCLI3346.1>
- Kwon, Y. O., Alexander, M. A., Bond, N. A., Frankignoul, C., Nakamura, H., Qiu, B., & Thompson, L. A. (2010). Role of the Gulf Stream and Kuroshio-Oyashio systems in large-scale atmosphere-Ocean interaction: a review. *Journal of Climate*, 23, 5206–5221.
- Lima, F. P., & Wethey, D. S. (2012). Three decades of high-resolution coastal sea surface temperatures reveal more than warming. *Nature Communications*, 3(1), 704. <https://doi.org/10.1038/ncomms1713>
- Liu, G. S., Cai, X. Y., Tong, F., Wang, L., & Zhang, X. M. (2014). Investigation of massive death of sea cucumber in artificial reef zone of Shuangdao Bay, Weihai. *Fisheries Information Strategy*, 29(02), 122–129.
- Luo, Y. M. (2016). Sustainability associated coastal eco-environmental problems and coastal science development in China (in Chinese). *Bulletin of the Chinese Academy of Sciences*, 31(10), 1133–1142.
- Manta, G., de Mello, S., Trinchin, R., Badagian, J., & Barreiro, M. (2018). The 2017 record marine heatwave in the Southwestern Atlantic Shelf. *Geophysical Research Letters*, 45, 12,449–12,456. <https://doi.org/10.1029/2018GL081070>
- Maynard, J. A., Turner, P. J., Anthony, K. R. N., Baird, A. H., Berkelmans, R., Eakin, C. M., et al. (2008). *ReefTemp*: An interactive monitoring system for coral bleaching using high-resolution SST and impoved stress predictors. *Geophysical Research Letters*, 35, L05603. <https://doi.org/10.1029/2007gl032175>
- McCabe, R. M., Hickey, B. M., Kudela, R. M., Lefebvre, K. A., Adams, N. G., Bill, B. D., et al. (2016). An unprecedented coastwide toxic algal bloom linked to anomalous ocean conditions. *Geophysical Research Letters*, 43, 366–376. <https://doi.org/10.1002/2016gl070023>
- Meehl, G. A., & Tebaldi, C. (2004). More intense, more frequent, and longer lasting heat waves in the 21st century. *Science*, 305(5686), 994–997. <https://doi.org/10.1126/science.1098704>
- Mills, K. E., Pershing, A. J., Brown, C. J., Chen, Y., Chiang, F. S., Holland, D. S., et al. (2013). Fisheries management in a changing climate: Lessons from the 2012 ocean heat wave in the Northwest Atlantic. *Oceanography*, 26, 191–195.
- Ministry of Agriculture of the People's Republic of China. Notice of the Ministry of Agriculture on printing and distributing the national marine ranching demonstration zone construction plan (2017–2025) (in Chinese). Retrieved from [http://jiuban.moa.gov.cn/zwlm/tzgg/tz/201712/t20171204\\_5961857.htm](http://jiuban.moa.gov.cn/zwlm/tzgg/tz/201712/t20171204_5961857.htm)
- Moore, G. W. K., Renfrew, I. A., & Pickart, R. S. (2012). Spatial distribution of air-sea heat fluxes over the sub-polar North Atlantic Ocean. *Geophysical Research Letters*, 39, L18806. <https://doi.org/10.1029/2012gl053097>
- Myers, T. A., Mechoso, C. R., Cesana, G. V., DeFlorio, M. J., & Waliser, D. E. (2018). Cloud feedback key to marine heatwave off Baja California. *Geophysical Research Letters*, 45, 4345–4352. <https://doi.org/10.1029/2018GL078242>
- Oliver, E. C., Benthuysen, J. C., Bindoff, N. L., Hobday, A. J., Holbrook, N. J., Mundy, C. N., & Perkins-Kirkpatrick, S. E. (2017). The unprecedented 2015/16 Tasman Sea marine heatwave. *Nature Communications*, 8(1), 16101. <https://doi.org/10.1038/ncomms16101>

- Oliver, E. C., Donat, M. G., Burrows, M. T., Moore, P. J., Smale, D. A., Alexander, L. V., et al. (2018). Longer and more frequent marine heatwaves over the past century. *Nature Communications*, 9(1), 1324. <https://doi.org/10.1038/s41467-018-03732-9>
- Oliver, E. C. J., Perkins-Kirkpatrick, S. E., Holbrook, N. J., & Bindoff, N. L. (2017). Anthropogenic and natural influences on record 2016 marine heat waves. *Bulletin of the American Meteorological Society*, 99, S44–S48.
- Rayner, N. A., Parker, D. E., Horton, E. B., Folland, C. K., Alexander, L. V., Rowell, D. P., et al. (2003). Global analyses of sea surface temperature, sea ice, and night marine air temperature since the late nineteenth century. *Journal of Geophysical Research*, 108(D14), 4407. <https://doi.org/10.1029/2002JD002670>
- Reynolds, R. W., Smith, T. M., Liu, C., Chelton, D. B., Casey, K. S., & Schlax, M. G. (2007). Daily high-resolution-blended analyses for sea surface temperature. *Journal of Climate*, 20(22), 5473–5496. <https://doi.org/10.1175/2007JCLI1824.1>
- Rhein, M., Rintoul, S. R., Aoki, S., Campos, E., Chambers, D., Feely, R. A., et al. (2013). Observations: Ocean. In T. F. Stocker, et al. (Eds.), *Climate change 2013: The physical science basis* (pp. 255–316). Cambridge: Cambridge University Press.
- Robinson, C. J. (2016). Evolution of the 2014–2015 sea surface temperature warming in the central west coast of Baja California, Mexico, recorded by remote sensing. *Geophysical Research Letters*, 43, 7066–7071. <https://doi.org/10.1002/2016GL069356>
- Rodrigues, R. R., Taschetto, A. S., Gupta, A. S., & Foltz, G. R. (2019). Common cause for severe droughts in South America and marine heatwaves in the South Atlantic. *Nature Geoscience*, 12(8), 620–626. <https://doi.org/10.1038/s41561-019-0393-8>
- Schlegel, R. W., Oliver, E. C., Wernberg, T., & Smit, A. J. (2017). Nearshore and offshore co-occurrence of marine heatwaves and cold-spells. *Progress in Oceanography*, 151, 189–205. <https://doi.org/10.1016/j.pocean.2017.01.004>
- Schmidtko, S., Stramma, L., & Visbeck, M. (2017). Decline in global oceanic oxygen content during the past five decades. *Nature*, 542(7641), 335–339. <https://doi.org/10.1038/nature21399>
- Selig, E. R., Casey, K. S., & Bruno, J. F. (2010). New insights into global patterns of ocean temperature anomalies: Implications for coral reef health and management. *Global Ecology and Biogeography*, 19, 397–411.
- Smale, D. A., Wernberg, T., Oliver, E. C., Thomsen, M., Harvey, B. P., Straub, S. C., et al. (2019). Marine heatwaves threaten global biodiversity and the provision of ecosystem services. *Nature Climate Change*, 9(4), 306–312. <https://doi.org/10.1038/s41558-019-0412-1>
- Song, N. Q., Wang, N., Lu, Y., & Zhang, J. R. (2016). Temporal and spatial characteristics of harmful algal blooms in the Bohai Sea during 1952–2014. *Continental Shelf Research*, 122, 77–84. <https://doi.org/10.1016/j.csr.2016.04.006>
- Sorte, C. J. B., Fuller, A., & Bracken, M. E. S. (2010). Impact of a simulated heat wave on composition of a marine community. *Oikos*, 119(12), 1909–1918. <https://doi.org/10.1111/j.1600-0706.2010.18663.x>
- Stott, P. A., Stone, D. A., & Allen, M. R. (2004). Human contribution to the European heatwave of 2003. *Nature*, 432, 61–64.
- Stramma, L., Johnson, G. C., Sprintall, J., & Mohrholz, Z. (2008). Expanding oxygen-minimum zones in the tropical oceans. *Science*, 320(5876), 655–658. <https://doi.org/10.1126/science.1153847>
- Tang, X., Wang, F., Chen, Y. L., & Li, M. K. (2009). Warming trend in northern East China Sea in recent four decades. *Chinese Journal of Oceanology and Limnology*, 27(2), 185–191. <https://doi.org/10.1007/s00343-009-9238-4>
- Taylor, K., Stouffer, R., & Meehl, G. (2012). An overview of CMIP5 and the experiment design. *Bulletin of the American Meteorological Society*, 93(4), 485–498. <https://doi.org/10.1175/BAMS-D-11-00094.1>
- Tencent News (2018). A large number of Dalian sea cucumbers were “hot” to death, resulting in a direct economic loss of RMB 68.7 billion. Retrieved from <https://new.qq.com/omn/20180805/20180805A1H3TU.html>
- Wang, Y. L., Wu, C. R., & Chao, S. Y. (2016). Warming and weakening trends of the Kuroshio during 1993–2013. *Geophysical Research Letters*, 43, 9200–9207. <https://doi.org/10.1002/2016GL069432>
- Wells, M. L., Trainer, V. L., Smayda, T. J., Karlson, B. S. Q., Trick, C. G., Kudela, R. M., et al. (2015). Harmful algal blooms and climate change: Learning from the past and present to forecast the future. *Harmful Algae*, 49, 68–93. <https://doi.org/10.1016/j.hal.2015.07.009>
- Wernberg, T., Bennett, S., Babcock, R. C., de Bettignies, T., Cure, K., Depczynski, M., et al. (2016). Climate-driven regime shift of a temperate marine ecosystem. *Science*, 353(6295), 169–172. <https://doi.org/10.1126/science.aad8745>
- Wernberg, T., Smale, D. A., Tuya, F., Thomsen, M. S., Langlois, T. J., de Bettignies, T., et al. (2013). An extreme climatic event alters marine ecosystem structure in a global biodiversity hotspot. *Nature Climate Change*, 3(1), 78–82. <https://doi.org/10.1038/nclimate1627>
- Whitney, F. A. (2015). Anomalous winter winds decrease 2014 transition zone productivity in the NE Pacific. *Geophysical Research Letters*, 42, 428–431. <https://doi.org/10.1002/2014GL062634>
- Wu, L. X., Cai, W. J., Zhang, L. P., Nakamura, H., Timmermann, A., & Joyce, T. (2012). Enhanced warming over the global subtropical western boundary currents. *Nature Climate Change*, 2(3), 161–166. <https://doi.org/10.1038/nclimate1353>
- Wu, R. H., Lin, J. M., & Li, B. (2017). Spatial and temporal variability of sea surface temperature in eastern marginal seas of China. *Advances in Meteorology*, 2016, 1–9.
- Yang, H. S., Huo, D., & Xu, Q. (2016). Views on modern marine ranching (in Chinese). *Oceanologia ET Limnologia Sinica*, 47, 1069–1074.
- Yang, H. S., Zhang, S. Y., Zhang, X. M., Chen, P. M., Tian, T., & Zhang, T. (2019). Strategic thinking on the construction of modern marine ranching in China (in Chinese). *Journal of Fisheries of China*, 43, 1255–1262.
- Yin, J., Overpeck, J., Peyser, C., & Stouffer, R. (2018). Big jump of record warm global mean surface temperature in 2014–2016 related to usually large oceanic heat releases. *Geophysical Research Letters*, 45, 1069–1078. <https://doi.org/10.1002/2017GL076500>
- Zhai, W. D., Zhao, H. D., Zheng, N., & Xu, Y. (2012). Coastal acidification in summer bottom oxygen-depleted waters in northwestern-northern Bohai Sea from June to August in 2011 (in Chinese). *Chinese Science Bulletin*, 57, 1062–1068.
- Zhao, H. D., Kao, S. J., Zhai, W. D., Zhang, K. P., Zheng, N., & Xu, X. M. (2017). Effects of stratification, organic matter remineralization and bathymetry on summertime oxygen distribution in the Bohai Sea, China. *Continental Shelf Research*, 134, 15–25. <https://doi.org/10.1016/j.csr.2016.12.004>
- Zhu, Z., Qu, P. P., Fu, F. X., Tennenbaum, N., Tatters, A. O., & Hutchins, D. A. (2017). Understanding the blob bloom: Warming increases toxicity and abundance of the harmful bloom diatom *Pseudo-nitzschia* in California coastal waters. *Harmful Algae*, 67, 36–43. <https://doi.org/10.1016/j.hal.2017.06.004>

## Erratum

Due to a typesetting error, the corrected version of this article was not published online. This corrected version has now been published in Wiley Online Library, and this may be considered the official version of record.